The Direct Synthesis of Hydrogen Peroxide Over Supported Pd-Based Catalysts: An Investigation into the Role of the Support and Secondary Metal Modifiers

Thomas Richards[1] · Richard J. Lewis[1] · David J. Morgan[1,2] · Graham J. Hutchings[1]

Abstract

The direct synthesis of H_2O_2 from molecular H_2 and O_2 over Pd-based catalysts, prepared via an industrially relevant, excess chloride co-impregnation procedure is investigated. Initial studies into the well-established PdAu system demonstrated the key role of Pd: Au ratio on catalytic activity, under conditions that have previously been found to be optimal for H_2O_2 formation. Further investigations using the optimal Pd: Au ratio identified the role of the catalyst support in controlling particle size and Pd oxidation state and thus catalytic performance. Subsequently, with an aim to replace Au with cheaper alternatives, the alloying of Pd with more abundant secondary metals is explored.

Graphical Abstract
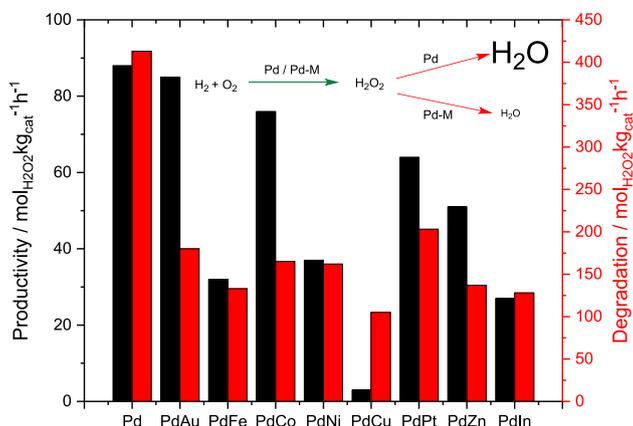
Thomas Richards and Richard J. Lewis are contributed equally to this work.

✉ Richard J. Lewis
    LewisR27@cardiff.ac.uk

✉ Graham J. Hutchings
    Hutch@cardiff.ac.uk

    Thomas Richards
    LewisR27@cardiff.ac.uk

1   Max Planck–Cardiff Centre on the Fundamentals of Heterogeneous Catalysis FUNCAT, Cardiff Catalysis Institute, School of Chemistry, Cardiff University, Main Building, Park Place, Cardiff CF10 3AT, UK

2   Harwell XPS, Research Complex at Harwell (RCaH), Didcot OX11 0FA, UK

🍀 Springer

1 Introduction

The direct synthesis of hydrogen peroxide (H_2O_2), a powerful and environmentally benign oxidising agent, offers an attractive alternative to the current means of production on an industrial scale, the anthraquinone oxidation process. Finding major application in industries that rely on its efficacy as a bleaching agent or its high oxidation potential, H_2O_2 is rapidly replacing commonly used stoichiometric reagents such as permanganate and perchlorate, reducing the build-up of unwanted by-products in product streams and minimising costs associated with energy intensive distillation and purification steps [1].

While the current industrial route to H_2O_2 production is highly efficient, economies of scale have precluded H_2O_2 manufacture at point of use. Instead H_2O_2 is typically shipped and stored at concentrations greatly exceeding those required by the end user, with the energy utilised in numerous purification and concentration steps effectively wasted once the H_2O_2 is diluted to required levels prior to use [2]. Furthermore, due to the low stability of H_2O_2, decomposing readily to H_2O at relatively mild temperatures or under an alkali pH, the use of acidic stabilizing agents is common [3]. While such additives prolong the shelf life of H_2O_2 they can promote reactor corrosion, decrease catalyst lifetime and necessitate the use of additional purification steps to remove such impurities from product streams, with the associated costs passed on to the end user [4].

Alternatively, the direct synthesis of H_2O_2 from molecular H_2 and O_2 has the potential to avoid many of the drawbacks associated with the anthraquinone oxidation process, allowing for the on-site manufacture of dilute streams of H_2O_2 [5]. Additionally, the in-situ production of H_2O_2 has been demonstrated to offer improved activity, compared to the use of preformed H_2O_2, in a range of selective chemical transformations, under reaction conditions where H_2O_2 is considered highly unstable [6–10]. With the enhanced performance of the in-situ approach possibly related to the avoidance of the acid stabilisers that are used to inhibit preformed H_2O_2 decomposition during transport and storage.

The incorporation of Au into supported Pd catalysts has been widely reported to result in a synergistic enhancement in catalytic activity towards H_2O_2 production [11, 12] (with extensive discussion of Au-based catalysis reported in [13]), likely occurring through a combination of isolation and electronic modification of Pd sites [12, 14]. Indeed, we have previously demonstrated that supported PdAu catalysts can offer near complete selectivity towards H_2O_2, in the absence of the acidic and halogenated promoters typically required to improve catalytic performance

of Pd-only materials [15–17]. While numerous methods to synthesize supported PdAu catalysts for H_2O_2 generation have been investigated, wet co-impregnation is perhaps both the most popular and most facile [18, 19]. However, this route to catalyst synthesis is typically somewhat hampered by poor dispersion of active metals, with a bimodal distribution of metal nanoparticles previously reported [8, 20, 21]. Indeed, detailed STEM-XEDS analysis has revealed a distinct relationship between particle size and elemental composition, with larger nanoparticles found to be Au-rich, while smaller nanoparticles are Pd-rich [22]. By comparison the preparation of supported PdAu catalysts via an excess chloride co-impregnation procedure has led to significantly improved catalytic efficacy compared to conventional wet co-impregnation analogues, with this attributed to a combination of increased nanoparticle size control, improved compositional uniformity and the formation of random alloy structures [23, 24].

With the performance of PdAu catalysts towards the direct synthesis and subsequent degradation of H_2O_2 well reported to be highly dependent on catalyst support [25] and a growing interest in the alloying of Pd with more abundant base metals [26–34] we now investigate the wider applicability of the excess chloride co-impregnation methodology to catalyst preparation.

2 Experimental

2.1 Catalyst Preparation

1% Au–Pd catalysts supported on a range of common oxide supports have been prepared (on a weight basis) by an excess chloride wet co-impregnation procedure, based on methodology previously reported in the literature [24], which has been shown to result in enhanced dispersion of precious metals, in particular Au, when compared to conventional wet co-impregnation methodologies. The procedure to produce 0.5%Pd–0.5%Au/TiO_2 (2 g) is outlined below, with a similar methodology utilised for all supported catalysts (see Table S.1 for further details).

Aqueous acidified $PdCl_2$ solution (1.667 mL, 0.58 M HCl, 6 mg mL^{-1}, Merck) and aqueous $HAuCl_4.3H_2O$ solution (0.8263 mL, 12.25 mg mL^{-1}, Strem Chemicals) were mixed in a 50 mL round bottom flask and heated to 60 °C with stirring (1000 rpm) in a thermostatically controlled oil bath, with total volume fixed to 16 mL using H_2O (HPLC grade). Upon reaching 65 °C, TiO_2 (1.98 g, Degussa, P25) was added over the course of 5 min with constant stirring. The resulting slurry was stirred at 60 °C for a further 15 min, following this the temperature was raised to 95 °C for 16 h to allow for complete evaporation of water. The resulting solid

was ground prior to heat treatment in a reductive atmosphere (flowing 5% H_2 / Ar, 400 °C, 4 h, 10 °C min^{-1}).

2.2 Catalyst Testing

Note 1: Reaction conditions used within this study operate under the flammability limits of gaseous mixtures of H_2 and O_2.

Note 2: The conditions used within this work for H_2O_2 synthesis and degradation have previously been investigated, with the presence of CO_2 as a diluent for reactant gases and a methanol co-solvent have identified as key to maintaining high catalytic efficacy towards H_2O_2 production [35].

2.3 Direct Synthesis of H_2O_2

Hydrogen peroxide synthesis was evaluated using a Parr Instruments stainless steel autoclave with a nominal volume of 100 mL and a maximum working pressure of 2000 psi. To test each catalyst for H_2O_2 synthesis, the autoclave was charged with catalyst (0.01 g) and solvent (5.6 g methanol and 2.9 g H_2O, Fischer Scientific, HPLC standard). The charged autoclave was then purged three times with 5% H_2/CO_2 (100 psi) before filling with 5% H_2/CO_2 to a pressure of 420 psi, followed by the addition of 25% O_2/ CO_2 (160 psi). The reaction was conducted at a temperature of 2 °C, for 0.5 h with stirring (1200 rpm). Reactant gases were not continuously supplied. H_2O_2 productivity was determined by titrating aliquots of the final solution after reaction with acidified $Ce(SO_4)_2$ (0.0085 M) in the presence of ferroin indicator. Catalyst productivities are reported as $mol_{H2O2}kg_{cat}^{-1}h^{-1}$.

Catalytic conversion of H_2 and selectivity towards H_2O_2 were determined using a Varian 3800 GC fitted with TCD and equipped with a Porapak Q column.

H_2 conversion (Eq. 1) and H_2O_2 selectivity (Eq. 2) are defined as follows:

$$H_2 \text{Conversion} (\%) = \frac{mmol_{H2(t(0))} - mmol_{H2(t(1))}}{mmol_{H2(t(0))}} \times 100 \tag{1}$$

$$H_2O_2 \text{ Selectivity} (\%) = \frac{H_2O_2 \text{detected (mmol)}}{H_2 \text{ consumed (mmol)}} \times 100 \tag{2}$$

2.4 Degradation of H_2O_2

Catalytic activity towards H_2O_2 degradation was determined in a similar manner to the direct synthesis activity of a catalyst. The autoclave was charged with methanol (5.6 g, Fischer Scientific, HPLC standard), H_2O_2 (50 wt. % 0.69 g, Merck), H_2O (2.21 g, Fischer Scientific HPLC standard) and catalyst (0.01 g), with the solvent composition

equivalent to a 4 wt. % H_2O_2 solution. From the solution 2 aliquots of 0.05 g were removed and titrated with acidified $Ce(SO_4)_2$ solution using ferroin as an indicator to determine an accurate concentration of H_2O_2 at the start of the reaction. The autoclave was pressurised with 5% H_2/CO_2 (420 psi). The reaction was conducted at a temperature of 2 °C, for 0.5 h with stirring (1200 rpm). After the reaction was complete the catalyst was removed from the reaction mixture and two aliquots of 0.05 g were titrated against the acidified $Ce(SO_4)_2$ solution using ferroin as an indicator. The degradation activity is reported as $mol_{H2O2}kg_{cat}^{-1} h^{-1}$.

Note 3: For both H_2O_2 direct synthesis and degradation experiments the reactor temperature was controlled using a HAAKE K50 bath/circulator using an appropriate coolant. Reactor temperature was maintained at 2 °C ± 0.2 °C throughout the course of the H_2O_2 synthesis and degradation reaction.

In all cases reactions were run multiple times, over multiple batches of catalyst, with the data being presented as an average of these experiments. The catalytic activity toward the direct synthesis and subsequent degradation of H_2O_2 was found to be consistent to within ± 2% on the basis of multiple reactions.

2.5 Catalyst Characterisation

A Thermo Scientific K-Alpha$^+$ photoelectron spectrometer was used to collect XP spectra utilising a micro-focused monochromatic Al K$_\alpha$ X-ray source operating at 72 W (6 mA × 12 kV). Samples were mounted by pressing into a copper sample holder using an IPA cleaned spatula and subsequently analysed using the 400 μm spot mode at pass energies of 40 and 150 eV for high-resolution and survey spectra with step sizes of 0.1 and 1 eV respectively. Charge compensation was performed using a combination of low energy electrons and argon ions, which resulted in a C(1 s) binding energy of 284.8 eV for the adventitious carbon present on all samples and all samples also showed a constant Ti(2p$_{3/2}$) of 458.5 eV. All data was processed using CasaXPS v2.3.24 [36] using a Shirley background, Scofield sensitivity factors [37] and an electron energy dependence of − 0.6 as recommended by the manufacturer. Peak fits were performed using a combination of Voigt-type functions and models derived from bulk reference samples where appropriate.

The bulk structure of the catalysts was determined by powder X-ray diffraction using a (θ-θ) PANalytical X'pert Pro powder diffractometer using a Cu K$_\alpha$ radiation source, operating at 40 keV and 40 mA. Standard analysis was carried out using a 40 min run with a back filled sample, between 2θ values of 10—80°. Phase identification was carried out using the International Centre for Diffraction Data (ICDD).

Total metal leaching from the supported catalyst was quantified via inductively coupled plasma mass spectrometry (ICP-MS). Post-reaction solutions were analysed using an Agilent 7900 ICP-MS equipped with I-AS auto-sampler. All samples were diluted by a factor of 10 using HPLC grade H_2O (1%HNO_3 and 0.5% HCl matrix). All calibrants were matrix matched and measured against a five-point calibration using certified reference materials purchased from Perkin Elmer and certified internal standards acquired from Agilent.

Brunauer–Emmett–Teller (BET) surface area measurements were conducted using a Quadrasorb surface area analyzer. A five-point isotherm of each material was measured using N_2 as the adsorbate gas. Samples were degassed at 250 °C for 2 h prior to the surface area being determined by five-point N_2 adsorption at − 196 °C, and data were analyzed using the BET method.

3 Results and Discussion

Our initial studies, under reaction conditions which have previously been optimised for H_2O_2 production [35] and using TiO_2 (P25) as the catalyst support, established the effect of Pd: Au ratio the catalytic activity of supported metal catalysts prepared via an excess-chloride methodology towards H_2O_2 synthesis and its subsequent degradation (Fig. 1). It should be noted that such a route to catalyst synthesis has previously been demonstrated to resulted in the enhanced dispersion of Au and the improved formation of PdAu random alloy morphologies [23]. In keeping with previous works into such analogously prepared PdAu catalysts
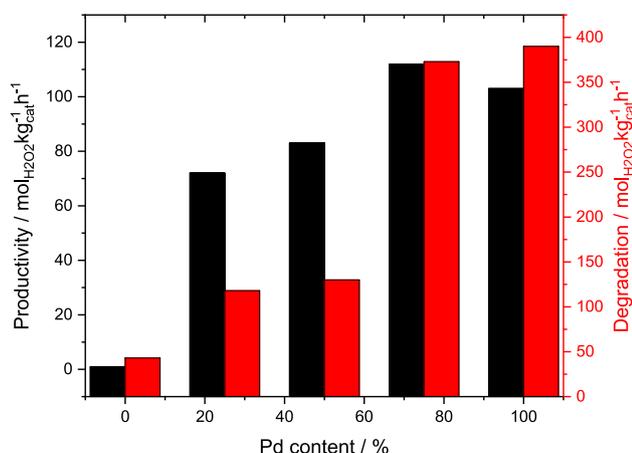
Fig. 1 Catalytic activity of 1%PdAu/TiO_2 catalysts towards the direct synthesis and subsequent degradation of H_2O_2, as a function of Au: Pd ratio. H_2O_2 direct synthesis reaction conditions: Catalyst (0.01 g), H_2O (2.9 g), MeOH (5.6 g), 5% H_2/CO_2 (420 psi), 25% O_2/CO_2 (160 psi), 0.5 h, 2 °C, 1200 rpm. H_2O_2 degradation reaction conditions: Catalyst (0.01 g), H_2O_2 (50 wt.% 0.68 g) H_2O (2.22 g), MeOH (5.6 g), 5% H_2 / CO_2 (420 psi), 0.5 h, 2 °C 1200 rpm

we observed a direct correlation between catalytic activity towards both the direct synthesis and subsequent degradation of H_2O_2 and Pd content [35]. Indeed, the H_2O_2 synthesis activity of the 1%Pd/TiO_2 (103 $mol_{H2O2}kg_{cat}^{-1}h^{-1}$) catalyst was observed to be significantly greater than that of the 0.5%Pd-0.5%Au/TiO_2 analogue (83 $mol_{H2O2}kg_{cat}^{-1}h^{-1}$), with apparent reaction rates reported in Table S.2. However, the bi-metallic catalyst was found to be far more selective, with H_2O_2 degradation rates (130 $mol_{H2O2}kg_{cat}^{-1}h^{-1}$) three times lower than the Pd-only catalyst (390 $mol_{H2O2}kg_{cat}^{-1}h^{-1}$). We have previously determined a strong correlation between the mean particle size of identically prepared PdAu catalysts and Pd content [35]. Indeed we have observed that the introduction of Pd into a supported Au nanoparticle results in a significant reduction in mean nanoparticle size, from approximately 8 nm in the case of the 1%Au/TiO_2 catalyst to below the limit of detection (approx. 1 nm) for the corresponding Pd-only analogue [35]. With the poor selectivity of smaller nanoparticles towards H_2O_2 previously reported [26, 38] we consider that the high degradation rates of the Pd-rich catalysts can be related, at least in part to differences in particle size across this series of catalysts. However, analysis via XPS also revealed the alloying of Au with Pd is also able to inhibit the formation of the large domains of Pd^0 that are present in the monometallic catalyst, despite exposure to a reductive heat treatment (5%H_2/Ar, 400 °C, 4 h). Indeed, the bi-metallic PdAu catalysts are observed to consist of a mix of both Pd^{2+} and Pd^0 (Figure S.1). The presence of these domains of mixed oxidation state has previously been identified as a key factor in dictating catalytic selectivity [39, 40] and as such we consider that the improved catalytic performance of the bi-metallic catalysts can be attributed to both a control of particle size and modification of Pd oxidation state.

With the clear enhancement in catalyst performance observed when Pd and Au are present at equal loading our subsequent studies established the efficacy of a series of supported PdAu catalysts, with a total metal loading of 1 wt.% and Pd: Au ratio of 1: 1 (wt/wt), towards the direct synthesis and subsequent degradation of H_2O_2 (Table 1). A strong dependency between catalytic performance and the choice of the support was observed, with the enhanced activity of the TiO_2 (85 $mol_{H2O2}kg_{cat}^{-1}h^{-1}$), Al_2O_3 (75 $mol_{H2O2}kg_{cat}^{-1}h^{-1}$), and SiO_2 (72 $mol_{H2O2}kg_{cat}^{-1}h^{-1}$) supported catalysts clear. The improved activity of these materials is further evidenced through comparison of initial reaction rate, where the contribution from competitive H_2O_2 degradation reactions is considered to be negligible (Table S.3). Previous studies have identified the limited H_2O_2 synthesis activity of PdAu nanoparticles immobilised on Al_2O_3 and SiO_2, compared to TiO_2 supported analogues when prepared via a conventional wet co-impregnation technique, *i.e.* in the absence of excess halide [41,

Table 1 Catalytic activity of supported PdAu catalysts towards the direct synthesis and subsequent degradation of H_2O_2, as a function of catalyst support

Catalyst	Productivity/mol-$_{H2O2}$kg$_{cat}^{-1}$ h^{-1}	H_2O_2 conc/wt.%	H_2 conv/%	H_2O_2 sel/%	Rate of reaction/mmol-$_{H2O2}$mmol$_{metal}^{-1}$ h^{-1}	Degradation/mol$_{H2O2}$kg-$_{cat}^{-1}$ h^{-1}
0.5%Pd/TiO$_2$	68	0.136	14	44	1.44×10^3	181
1%Pd/TiO$_2$	88	0.178	17	38	9.24×10^2	413
0.5%Pd-0.5%Au/TiO$_2$	85	0.170	19	54	1.22×10^3	180
0.5%Pd-0.5%Au/ Al$_2$O$_3$	75	0.150	13	29	1.03×10^3	196
0.5%Pd-0.5%Au/ SiO$_2$	72	0.145	8	53	9.97×10^2	158
0.5%Pd-0.5%Au/ZrO$_2$	10	0.020	7	43	9.6×10^1	94
0.5%Pd-0.5%Au/CeO$_2$	15	0.030	8	45	2.04×10^2	130
0.5%Pd-0.5%Au/Nb$_2$O$_5$	11	0.023	5	34	1.48×10^2	242

H_2O_2 direct synthesis reaction conditions: Catalyst (0.01 g), H_2O (2.9 g), MeOH (5.6 g), 5% H_2/CO_2 (420 psi), 25% O_2/CO_2 (160 psi), 0.5 h, 2 °C, 1200 rpm. H_2O_2 degradation reaction conditions: Catalyst (0.01 g), H_2O_2 (50 wt.% 0.68 g) H_2O (2.22 g), MeOH (5.6 g), 5% H_2/CO_2 (420 psi), 0.5 h, 2 °C 1200 rpm. Note 1: All catalyst exposed to a reductive heat treatment (5%H_2/Ar, 4 h, 400 °C, 10°Cmin^{-1}) prior to use. Note 2: Reaction rates upon are calculated based on theoretical metal content.

42]. However, we have demonstrated that by synthesising these catalysts via an excess chloride route it is possible to enhance the activity of the Al$_2$O$_3$ and SiO$_2$ supported materials, so that H_2O_2 synthesis rates are comparable to the TiO$_2$ analogue. Meanwhile ICP-MS analysis of post-H_2O_2 synthesis reactions revealed the high stability of the supported catalysts (Table S.4). As expected, investigation of the activity of the support materials, in the absence of the precious metals, identified the limited contribution to both H_2O_2 production and degradation (Table S.5), indicating that the observed activity of the catalysts is associated with the precious metal nanoparticles.

Numerous studies have identified that the choice of catalyst support may have a major effect on catalytic performance, influencing the degree of alloy formation, nanoparticle morphology and metal dispersion [25, 41, 43]. Indeed, we have shown that the isoelectric point of the support (*i.e.,* the pH at which the surface has zero net charge and an indication of catalyst acidity/basicity), is a crucial factor in determining the performance of PdAu catalysts prepared via a conventional wet co-impregnation methodology, with supports of low isoelectric point reported to offer enhanced rates of H_2O_2 synthesis [25]. While it may be expected that the use of supports of lower isoelectric point and therefore of greater acidity, may lead to an enhanced catalytic performance we do not observe such a trend in activity/selectivity (Table S.6). It should be noted that we have previously demonstrated that when many of the materials used as supports in this work are used as solid additives for a supported AuPd catalyst there is a negligible effect on catalytic performance [44]. This in addition to the negligible activity of all support materials to degrade H_2O_2 (Table S.5) may be indicative of the limited role of support acidity/basicity on catalytic performance.

Analysis of the supported PdAu catalysts via X-ray diffraction (Figure S.2.A-F) indicates that for a minority of the catalysts metal dispersion may be poor, with clear reflections associated with precious metals observed in the as-prepared CeO$_2$ and SiO$_2$ supported catalysts. This is despite the high surface area of the latter material (314 m^{2}g^{-1}, surface areas as determined via BET reported in Table S.7) and is in keeping with our previously investigations into PdAu catalysts prepared on a range of oxide supports via a conventional wet co-impregnation route [23, 25, 42, 45].

As discussed previously the role of Pd oxidation state in controlling catalytic performance towards the direct synthesis of H_2O_2 has been well studied [46, 47], with the formation of domains of mixed Pd oxidation state suggested to be a key factor in achieving enhanced catalytic efficacy towards the direct synthesis of H_2O_2. Indeed, catalysts consisting of such domains have been reported to offer improved performance compared to those that consist predominantly of Pd^{2+} or Pd^0 [39, 40]. Analysis of the supported PdAu catalysts via XPS reveals that the choice of catalyst support can significantly alter surface Pd speciation (Figure S.3), despite exposure to a reductive heat treatment prior to use (5%H_2/Ar, 400 °C, 4 h, 10 °C min^{-1}) all catalysts studied were observed to consist of a mixture of Pd oxidation states, with the exception of the 0.5%Pd-0.5%Au/ZrO$_2$ catalyst, which was found to exist entirely of Pd^0. Interestingly, analysis of the 0.5%Pd-0.5%Au/CeO$_2$ catalyst revealed a major proportion of Pd exits as neither PdO or Pd^0, but rather as PdCl$_x$, which further highlights the key role of the support in determining Pd speciation. Additionally, it should be noted that the weak signals in the Pd3d XPS spectra for both the 0.5%Pd–0.5%Au/SiO$_2$ and 0.5%Pd–0.5%Au/Al$_2$O$_3$ catalysts preclude a reliable determination of Pd speciation, although it is possible to infer that Pd^{2+} is the dominant

species, given the larger signal intensity in the 336–337 eV range for these catalysts. The weak XPS signals are consistent with our XRD analysis, which indicates the presence of larger metal nanoparticles in the Al_2O_3 and SiO_2 supported catalysts (Figure S.2.A and C). However, this clearly does not limit catalytic performance to any large extent, with both catalysts offering reasonable activity towards H_2O_2 production, with synthesis rates of 75 $mol_{H2O2}kg_{cat}^{-1}h^{-1}$ and 72 $mol_{H2O2}kg_{cat}^{-1}h^{-1}$ reported for the Al_2O_3 and SiO_2 based materials, comparable to that observed over the TiO_2 supported analogue (85 $mol_{H2O2}kg_{cat}^{-1}h^{-1}$).

In recent years a growing focus has been placed on the use non-precious metal containing Pd-based alloys for the direct synthesis of H_2O_2 including, but not limited to Pb [48], Sn [26, 32], Ni [28], Zn [34], Ga [30], Cu [27], Co [49] and Fe [7, 10, 50]. With these previous studies in mind and with an aim to reduce financial costs associated with catalyst synthesis, we subsequently investigated the efficacy of alloying Pd with a range of abundant transition metals. With catalytic performance towards the direct synthesis and subsequent degradation of H_2O_2 over a standard 0.5 h reaction reported in Table 2 and determination of initial reaction rates reported in Table S.8. The introduction of a range of transition metals was found to inhibit H_2O_2 degradation rates considerably, compared to the 1%Pd/TiO_2 catalyst (413 $mol_{H2O2}kg_{cat}^{-1}h^{-1}$), with a corresponding increase in catalytic selectivity towards H_2O_2 during the direct synthesis reaction also observed for many catalyst formulations. In particular the addition of Co (56% H_2O_2 selectivity) and Zn (68% H_2O_2 selectivity) was observed to result in a considerable improvement in catalytic selectivity towards H_2O_2. Indeed, for all of the bimetallic Pd-based catalysts, with the exception of the 0.5%Pd-0.5%Pt/TiO_2 analogue, H_2O_2

degradation rates were found to be considerably lower than that observed over the 0.5%Pd-0.5%Au/TiO_2 catalyst (180 $mol_{H2O2}kg_{cat}^{-1}h^{-1}$). However, despite the improved selectivity of these bi-metallic Pd-based catalysts, a corresponding improvement in H_2O_2 synthesis activity was not observed. While not as active as the 1%Pd/TiO_2 or 0.5%Pd-0.5%Au/TiO_2 catalysts to H_2O_2 synthesis we consider that the PdCo (76 $mol_{H2O2}kg_{cat}^{-1}h^{-1}$) and PdZn (51 $mol_{H2O2}kg_{cat}^{-1}h^{-1}$) formulations in particular to be of interest and to warrant further future investigation.

BET analysis of the Pd-based catalysts (Table S.9) indicates differences in catalytic performance cannot be associated with changes in catalyst surface area, while subsequent analysis via XRD (Figure S.4 A-B) reveals that, as with our earlier studies (Figure S.2.F), the formation of large metal nanoparticles may be avoided through the careful selection of catalyst support. Further evaluation via XPS (Figure S.5) demonstrates that the incorporation of all secondary metals significantly enhances the proportion of Pd^{2+} compared to the Pd-only catalyst, which was found to consist entirely of Pd^0 (Figure S.1). This correlates well with the observed decrease in H_2O_2 degradation rates and improvements in H_2O_2 selectivity upon the introduction of secondary metals.

It should be noted that while the 0.5%Pd-0.5%Cu/TiO_2 catalyst was found to consist of both Pd^{2+} and Pd^0 species, which has typically been found to correlate well with improved catalytic performance, both H_2O_2 production (3 $mol_{H2O2}kg_{cat}^{-1}h^{-1}$) and subsequent degradation activity (105 $mol_{H2O2}kg_{cat}^{-1}h^{-1}$) was found to be limited. Additionally, determination of H_2 conversion indicates a significant reduction in this metric with the introduction of Cu into a supported Pd catalyst (3% H_2 conversion). As such we consider Cu to act as an inhibitor of catalytic activity,

Table 2 Catalytic activity of bimetallic Pd-based catalysts towards the direct synthesis and subsequent degradation of H_2O_2, as a function secondary metal

Catalyst	Productivity/$mol_{H2O2}kg_{cat}^{-1}h^{-1}$	H_2O_2 conc./wt.%	H_2 conv./%	H_2O_2 sel. /%	Rate of reaction/$mmol_{H2O2}mmol_{metal}^{-1}h^{-1}$	Degradation/$mol_{H2O2}kg_{cat}^{-1}h^{-1}$
0.5%Pd/TiO_2	68	0.136	14	44	1.44×10^3	181
1%Pd/TiO_2	88	0.178	17	38	9.24×10^2	413
0.5%Pd-0.5%Au/TiO_2	85	0.170	19	54	1.22×10^3	180
0.5%Pd-0.5%Fe/ TiO_2	32	0.065	8	39	2.24×10^2	133
0.5%Pd-0.5%Co/ TiO_2	76	0.152	24	56	5.72×10^2	165
0.5%Pd-0.5%Ni/ TiO_2	37	0.074	6	32	2.81×10^2	162
0.5%Pd-0.5%Cu/ TiO_2	3	0.005	5	21	2.7×10^1	105
0.5%Pd-0.5%Pt/ TiO_2	64	0.123	29	41	4.62×10^2	203
0.5%Pd-0.5%Zn/TiO_2	51	0.102	15	68	4.09×10^2	137
0.5%Pd-0.5%In/TiO_2	27	0.050	8	53	2.07×10^2	128

H_2O_2 direct synthesis reaction conditions: Catalyst (0.01 g), H_2O (2.9 g), MeOH (5.6 g), 5% H_2/CO_2 (420 psi), 25% O_2/CO_2 (160 psi), 0.5 h, 2 °C, 1200 rpm. H_2O_2 degradation reaction conditions: Catalyst (0.01 g), H_2O_2 (50 wt.% 0.68 g) H_2O (2.22 g), MeOH (5.6 g), 5%H_2/CO_2 (420 psi), 0.5 h, 2 °C 1200 rpm. Note: All catalyst exposed to a reductive heat treatment (5%H_2/Ar, 4 h, 400 °C, 10 °C min-1) prior to use.

with these observations in keeping with numerous previous studies [7, 51–53].

4 Conclusion

The ability of Au incorporation to improve the catalytic activity of Pd-based catalysts towards the direct synthesis of H_2O_2 is established utilising TiO_2 (P25)-supported materials, prepared via an excess chloride wet co-impregnation procedure. Unlike in earlier studies that focussed on conventional wet co-impregnation routes, which avoid the use of high quantities of HCl during catalyst synthesis, a direct correlation between Pd content and H_2O_2 degradation rate was observed. This is attributed to the significant decrease in particle size that accompanies a shift towards Pd-rich compositions. Utilizing a range of catalyst supports and an optimal Pd: Au ratio the applicability of the excess chloride route to catalyst preparation was subsequently investigated, with the choice of catalyst support shown to control Pd speciation and nanoparticle size, and subsequently catalytic performance. Finally, the replacement of Au with a number of base metals was found to inhibit H_2O_2 degradation activity significantly, achieving degradation rates generally less than the corresponding PdAu catalyst and substantially less than the Pd-only analogue. While the catalytic performance of these Pd-based bimetallic catalysts towards H_2O_2 synthesis was found to be lower than both the Pd-only and PdAu catalysts the potential cost savings that may result from Au replacement with cheaper alternative metals is highly attractive and in particular we consider that the PdCo and PdZn catalysts to represent a promising basis for further exploration.

Supplementary Information The online version contains supplementary material available at https://doi.org/10.1007/s10562-022-03967-8.

Author Contributions T.R. and R.J.L conducted catalytic synthesis, testing and data analysis. T.R, R.J.L and D.J.M conducted catalyst characterisation and corresponding data processing. R.J.L and G.J.H contributed to the design of the study and provided technical advice and result interpretation. R.J.L wrote the manuscript and Supplementary Information, with all authors commenting on and amending both documents. All authors discussed and contributed to the work.

Data Availability All data generated or analysed during this study are included in this article and the corresponding supplementary information.

Declarations

Conflict of interest The authors declare no competing interests.

References

1. Lewis RJ, Hutchings GJ (2019) Recent advances in the direct synthesis of H_2O_2. ChemCatChem 11:298–308
2. Li H, Zheng B, Pan Z, Zong B, Qiao M (2018) Advances in the slurry reactor technology of the anthraquinone process for H_2O_2 production. Front Chem Sci Eng 12:124–131
3. Wegner P (2003). Hydrogen peroxide stabilizer and resulting product and applications US20050065052A15
4. Gao G, Tain Y, Gong X, Pan Z, Yong K, Zong B (2020) Advances in the production technology of hydrogen peroxide. Chin J. Catal 41:1039–1047
5. Edwards JK, Freakley SJ, Lewis RJ, Pritchard JC, Hutchings GJ (2015) Advances in the direct synthesis of hydrogen peroxide from hydrogen and oxygen. Catal Today 248:3–9
6. Crombie CM, Lewis RJ, Taylor RL, Morgan DJ, Davies TE, Folli A, Murphy DM, Edwards JK, Qi J, Jiang H, Kiely CJ, Liu X, Skjøth-Rasmussen MS, Hutchings GJ (2021) Enhanced selective oxidation of Benzyl alcohol via In Situ H_2O_2 production over supported Pd-based catalysts. ACS Catal 11:2701–2714
7. Crombie CM, Lewis RJ, Kovačič D, Morgan DJ, Slater TJA, Davies TE, Edwards JK, Skjøth-Rasmussen MS, Hutchings GJ (2021) The selective oxidation of cyclohexane via In-situ H_2O_2 production over supported Pd-based catalysts. Catal Lett 151:2762–2774
8. Crombie CM, Lewis RJ, Kovačič D, Morgan DJ, Davies TE, Edwards JK, Skjøth-Rasmussen MS, Hutchings GJ (2021) The influence of reaction conditions on the oxidation of cyclohexane via the in-situ production of H_2O_2. Catal Lett 151:164–171
9. Jin Z, Wang L, Zuidema E, Mondal K, Zhang M, Zhang J, Wang C, Meng X, Yang H, Mesters C, Xiao F (2020) Hydrophobic zeolite modification for in situ peroxide formation in methane oxidation to methanol. Science 367:193–197
10. Santos A, Lewis RJ, Morgan DJ, Davies TE, Hampton E, Gaskin P, Hutchings GJ (2021) The degradation of phenol via in situ H_2O_2 production over supported Pd-based catalysts. Catal Sci Technol 11:7866–7874
11. Wilson NM, Priyadarshini P, Kunz S, Flaherty DW (2018) Direct synthesis of H_2O_2 on Pd and AuxPd1 clusters: understanding the effects of alloying Pd with Au. J Catal 357:163–175
12. Li J, Ishihara T, Yoshizawa K (2011) Theoretical revisit of the direct synthesis of H_2O_2 on Pd and Au@Pd surfaces: a comprehensive mechanistic study. J Phys Chem C 115:25359–25367
13. Hashmi ASK, Hutchings GJ (2006) Gold catalysis. Angew Chem Int Ed 45:7896–7936

14. Staykov A, Kamachi T, Ishihara T, Yoshizawa K (2008) Theoretical study of the direct synthesis of H_2O_2 on Pd and Pd/Au surfaces. J Phys Chem C 112:19501–19505

15. Edwards JK, Solsona B, Ntainjua EN, Carley AF, Herzing AA, Kiely CJ, Hutchings GJ (2009) Switching off hydrogen peroxide hydrogenation in the direct synthesis process. Science 323:1037–1041

16. Choudhary V, Samanta C (2006) Role of chloride or bromide anions and protons for promoting the selective oxidation of H_2 by O_2 to H_2O_2 over supported Pd catalysts in an aqueous medium. J Catal 238:28–38

17. Choudhary VR, Samanta C, Jana P (2007) Hydrogenation of hydrogen peroxide over palladium/carbon in aqueous acidic medium containing different halide anions under static/flowing hydrogen. Ind. Eng. Chem. Res. 46:3237–3242

18. Lewis RJ, Ueura K, Fukuta Y, Freakley SJ, Kang L, Wang R, He Q, Edwards JK, Morgan DJ, Yamamoto Y, Hutchings GJ (2019) The direct synthesis of H_2O_2 using TS-1 supported catalysts. ChemCatChem 11:1673–1680

19. Pritchard JC, He Q, Ntainjua EN, Piccinini M, Edwards JK, Herzing AA, Carley AF, Moulijn JA, Kiely CJ, Hutchings GJ (2010) The effect of catalyst preparation method on the performance of supported Au-Pd catalysts for the direct synthesis of hydrogen peroxide. Green Chem 12:915–921

20. Hutchings GJ, Kiely CJ (2013) Strategies for the synthesis of supported gold palladium nanoparticles with controlled morphology and composition. Acc Chem Res 46:1759–1772

21. Edwards JK, Carley AF, Herzing AA, Kiely CJ, Hutchings GJ (2008) Direct synthesis of hydrogen peroxide from H_2 and O_2 using supported Au–Pd catalysts. Faraday Discuss 138:225–239

22. Herzing AA, Watanabe M, Edwards JK, Conte M, Tang Z, Hutchings GJ, Kiely CJ (2008) Energy dispersive X-ray spectroscopy of bimetallic nanoparticles in an aberration corrected scanning transmission electron microscope. Faraday Discuss 138:337–351

23. Sankar M, He Q, Morad M, Pritchard J, Freakley SJ, Edwards JK, Taylor SH, Morgan DJ, Carley AF, Knight DW, Kiely CJ, Hutchings GJ (2012) Synthesis of stable ligand-free gold-palladium nanoparticles using a simple excess anion method. ACS Nano 6:6600–6613

24. Brehm J, Lewis RJ, Morgan DJ, Davies TE, Hutchings GJ (2021) The Direct synthesis of hydrogen peroxide over AuPd nanoparticles: an investigation into metal loading. Catal Lett 152:254–262

25. Ntainjua EN, Edwards JK, Carley AF, Lopez-Sanchez JA, Moulijn JA, Herzing AA, Kiely CJ, Hutchings GJ (2008) The role of the support in achieving high selectivity in the direct formation of hydrogen peroxide. Green Chem 10:1162–1169

26. Freakley SJ, He Q, Harrhy JH, Lu L, Crole DA, Morgan DJ, Ntainjua EN, Edwards JK, Carley AF, Borisevich AY, Kiely CJ, Hutchings GJ (2016) Palladium-tin catalysts for the direct synthesis of H_2O_2 with high selectivity. Science 351:965–968

27. Wang Y, Pan H, Lin Q, Shi Y, Zhang J (2020) Synthesis of Pd-M@HCS(M = Co, Ni, Cu) bimetallic catalysts and their catalytic performance for direct synthesis of H_2O_2. Catalysts 10:303

28. Crole DA, Underhill R, Edwards JK, Shaw G, Freakley SJ, Hutchings GJ, Lewis RJ (2020) The direct synthesis of hydrogen peroxide from H_2 and O_2 using PdNi/TiO$_2$ catalysts. Phil Trans R Soc 378:20200062

29. Ding D, Xu X, Tian P, Liu X, Xu J, Han Y (2018) Promotional effects of Sb on Pd-based catalysts for the direct synthesis of hydrogen peroxide at ambient pressure. Chin J Catal 39:673–681

30. Wang S, Lewis RJ, Doronkin DE, Morgan DJ, Grunwaldt J, Hutchings GJ, Behrens S (2020) The direct synthesis of hydrogen peroxide from H_2 and O_2 using Pd-Ga and Pd-In catalysts. Catal Sci Technol 10:1925–1932

31. Han G, Xiao X, Hong J, Lee K, Park S, Ahn J, Lee K, Yu T (2020) Tailored palladium-platinum nanoconcave cubes as high performance catalysts for the direct synthesis of hydrogen peroxide. ACS Appl Mater Interfaces 12:6328–6335

32. Doronkin DE, Wang S, Sharapa DI, Deschner BJ, Sheppard TL, Zimina A, Studt F, Dittmeyer R, Behrens S, Grunwaldt J (2020) Dynamic structural changes of supported Pd, PdSn, and PdIn nanoparticles during continuous flow high pressure direct H_2O_2 synthesis. Catal. Sci. Technol. 10:4726–4742

33. Wilson NM, Schröder J, Priyadarshini P, Bregante DT, Kunz S, Flaherty DW (2018) Direct synthesis of H_2O_2 on PdZn nanoparticles: The impact of electronic modifications and heterogeneity of active sites. J Catal 368:261–274

34. Wang S, Gao K, Li W, Zhang J (2017) Effect of Zn addition on the direct synthesis of hydrogen peroxide over supported palladium catalysts. Appl Catal A 531:89–95

35. Santos A, Lewis RJ, Malta G, Howe AGR, Morgan DJ, Hampton E, Gaskin P, Hutchings GJ (2019) Direct synthesis of hydrogen peroxide over Au–Pd supported nanoparticles under ambient conditions. Ind Eng Chem Res 58:12623–12631

36. Fairley N, Fernandez V, Richard-Plouet M, Guillot-Deudon C, Walton J, Smith E, Flahaut D, Greiner M, Biesinger M, Tougaard S, Morgan D, Baltrusaitis J (2021) Systematic and collaborative approach to problem solving using X-ray photoelectron spectroscopy. Appl. Surf. Sci. 5:100112

37. Scofield JH (1976) Hartree-Slater subshell photoionization cross-sections at 1254 and 1487 eV. J Electron Spectrosc Relat Phenom 8:129–137

38. Williams C, Carter JH, Dummer NF, Chow YK, Morgan DJ, Yacob S, Serna P, Willock DJ, Meyer RJ, Taylor SH, Hutchings GJ (2018) Selective oxidation of methane to methanol using supported AuPd catalysts prepared by stabilizer-free sol-immobilization. ACS Catal 8:2567–2576

39. Ouyang L, Tian P, Da G, Xu X, Ao C, Chen T, Si R, Xu J, Han Y (2015) The origin of active sites for direct synthesis of H_2O_2 on Pd/TiO$_2$ catalysts: interfaces of Pd and PdO domains. J Catal 321:70–80

40. Gong X, Lewis RJ, Zhou S, Morgan DJ, Davies TE, Liu X, Kiely CJ, Zong B, Hutchings GJ (2020) Enhanced catalyst selectivity in the direct synthesis of H_2O_2 through Pt incorporation into TiO$_2$ supported AuPd catalysts. Catal Sci Technol 10:4635–4644

41. Edwards JK, Thomas A, Solsona BE, Landon P, Carley AF, Hutchings GJ (2007) Comparison of supports for the direct synthesis of hydrogen peroxide from H_2 and O_2 using Au-Pd catalysts. Catal Today 122:397–402

42. Edwards JK, Parker SF, Pritchard J, Piccinini M, Freakley SJ, He Q, Carley AF, Kiely CJ, Hutchings GJ (2013) Effect of acid pre-treatment on AuPd/SiO$_2$ catalysts for the direct synthesis of hydrogen peroxide. Catal Sci Technol 3:812–818

43. Edwards JK, Thomas A, Carley AF, Herzing AA, Kiely CJ, Hutchings GJ (2008) Au–Pd supported nanocrystals as catalysts for the direct synthesis of hydrogen peroxide from H_2 and O_2. Green Chem 10:388–394

44. Lewis RJ, Edwards JK, Freakley SJ, Hutchings GJ (2017) Solid acid additives as recoverable promoters for the direct synthesis of hydrogen peroxide. Ind Eng Chem Res 56:13287–13293

45. Solsona BE, Edwards JK, Landon P, Carley AF, Herzing AA, Kiely CJ, Hutchings GJ (2006) Direct synthesis of hydrogen peroxide from H_2 and O_2 using Al$_2$O$_3$ supported Au-Pd catalysts. Chem Mater 18:2689–2695

46. Blanco-Brieva G, Cano-Serrano E, Campos-Martin JM, Fierro JLG (2004) Direct synthesis of hydrogen peroxide solution with palladium-loaded sulfonic acid polystyrene resins. Chem. Commun. 10:1184–1185

47. Gaikwad AG, Sansare SD, Choudhary VR (2002) Direct oxidation of hydrogen to hydrogen peroxide over Pd-containing fluorinated

or sulfated Al_2O_3, ZrO_2, CeO_2, ThO_2, Y_2O_3 and Ga_2O_3 catalysts in stirred slurry reactor at ambient conditions. J Mol Catal A: Chem 181:143–149

48. Cao K, Yang H, Bai S, Xu Y, Yang C, Wu Y, Xie M, Cheng T, Shao Q, Huang X (2021) Efficient direct H_2O_2 synthesis enabled by PdPb nanorings via inhibiting the O-O bond cleavage in O_2 and H_2O_2. ACS Catal 11:1106–1118

49. Nazeri H, Chermahini AN, Mohammadbagheri Z, Prato M (2021) Direct production of hydrogen peroxide over bimetallic CoPd catalysts: Investigation of the effect of Co addition and calcination temperature. In Press, Green Energy Environ

50. Underhill R, Douthwaite M, Lewis RJ, Miedziak PJ, Armstrong RD, Morgan DJ, Freakley SJ, Davies TE, Folli A, Murphy DM, He Q, Akdim O, Edwards JK, Hutchings GJ (2021) Ambient base-free glycerol oxidation over bimetallic $PdFe/SiO_2$ by in situ generated active oxygen species. Res Chem Intermed 47:303–324

51. Alotaibi F, Al-Mayman S, Alotaibi M, Edwards JK, Lewis RJ, Alotaibi R, Hutchings GJ (2019) Direct synthesis of hydrogen peroxide using Cs-containing Heteropolyacid-supported Palladium-copper catalysts. Catal Lett 149:998–1006

52. Ab Rahim MH, Armstrong RD, Hammond C, Dimitratos N, Freakley SJ, Forde MM, Morgan DJ, Lalev G, Jenkins RL, Lopez-Sanchez JA, Taylor SH, Hutchings GJ (2016) Low temperature selective oxidation of methane to methanol using titania supported gold palladium copper catalysts. Catal Sci Technol 6:3410–3418

53. Joshi AM, Delgass WN, Thomson KT (2007) Investigation of Gold−Silver, Gold−Copper, and Gold−Palladium dimers and trimers for hydrogen peroxide formation from H_2 and O_2. J Phys Chem C 111:7384–7395